Supplementary Information (SI) for Energy & Environmental Science.
This journal is © The Royal Society of Chemistry 2024

Stabilizing aluminum metal anode by a polymer coating-enabled exchange current regulation

Sichen Gu[a,b,c], Wanli Nie [a,b], Qiao Meng [a], Xinming Chen [a], Jiameng Zhang [a], Yun Cao [c], Wei Lv[c*]

[a.] *Department of Materials Science, Shenzhen MSU-BIT University, Shenzhen 518172, China*

[b.] *Laboratory for Advanced Materials and Batteries, Institute of Advanced Interdisciplinary Technology, Shenzhen MSU-BIT University, Shenzhen 518172, China*

[c.] *Shenzhen Key Laboratory for Graphene-based Materials and Engineering Laboratory for Functionalized Carbon Materials, Tsinghua Shenzhen International Graduate School, Tsinghua University, Shenzhen 518071, China, E-mail: lv.wei@sz.tsinghua.edu.cn*

Correspondence and requests for materials should be addressed to W. Lv. (lv.wei@sz.tsinghua.edu.cn)

Supplementary Figures

Fig. S1 a) pristine PDMS coin and PDMS coin socked in the IL for b) 24 h, c) 48 h, d) 72 h, and e) 96 h.

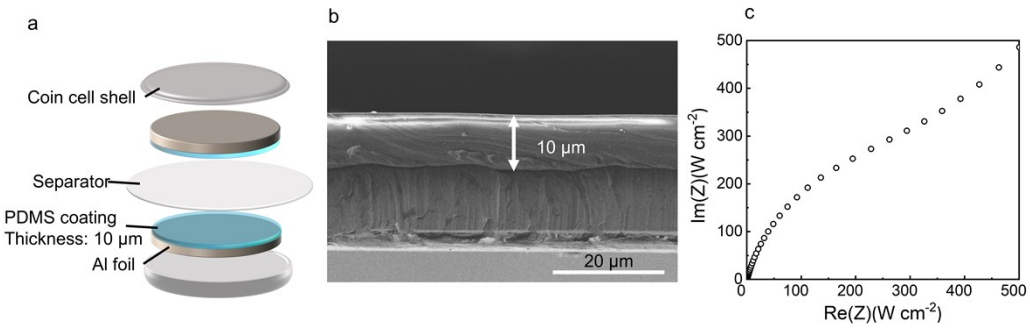

Fig. S2 a) Schematic of the symmetrical cell with PDMS-coated Al foil. b) SEM for the cross-section view of PDMS-coated Al foil. c) Zooming up of the impedance spectra of the symmetrical Al||Al cell

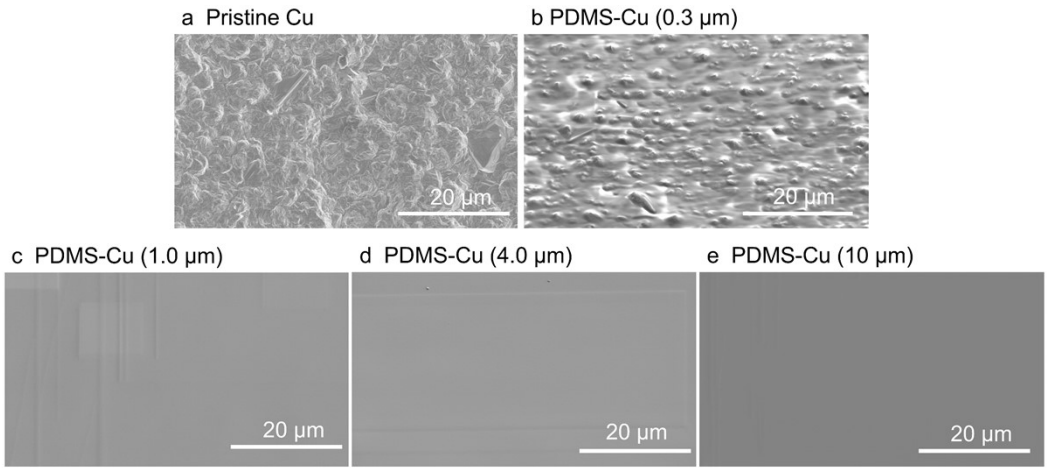

Fig. **S3** SEM image of the surface morphology of the a) pristine Cu and b-e) the PDMS-Cu with the varied thickness.

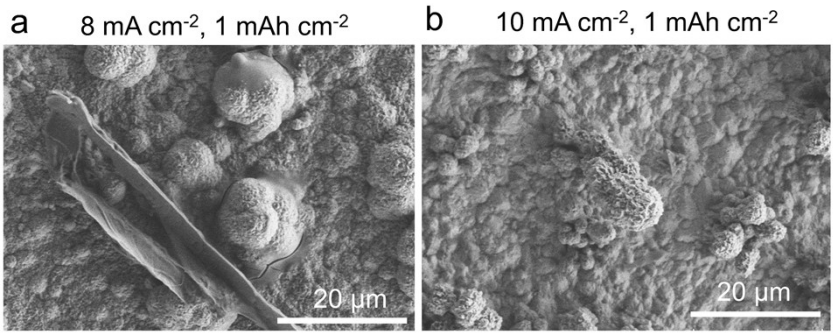

Fig. S4 The Al deposit on the Cu foil under the current density of 8 mA cm^{-2} and 10 mA cm^{-2}.

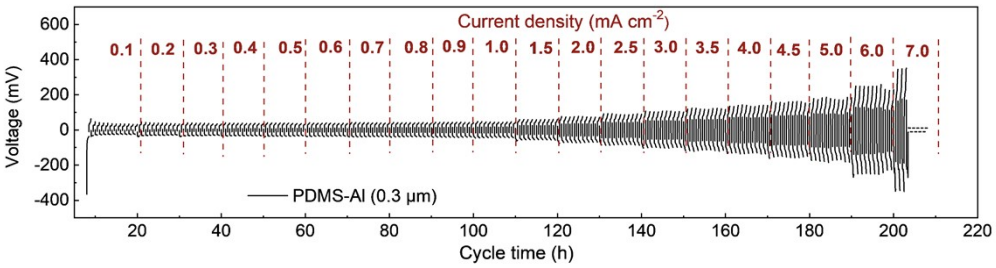

Fig. S5 The galvanostatic charge and discharge curves of the symmetrical cells with the PDMS-Al (0.3 μm).

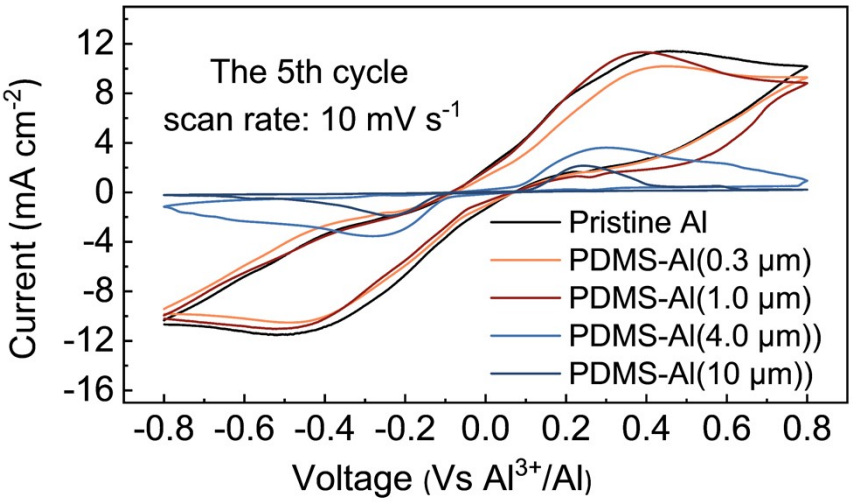

Fig. S6 The CV curves of the symmetrical cells with pristine Al and PDMS-Al.

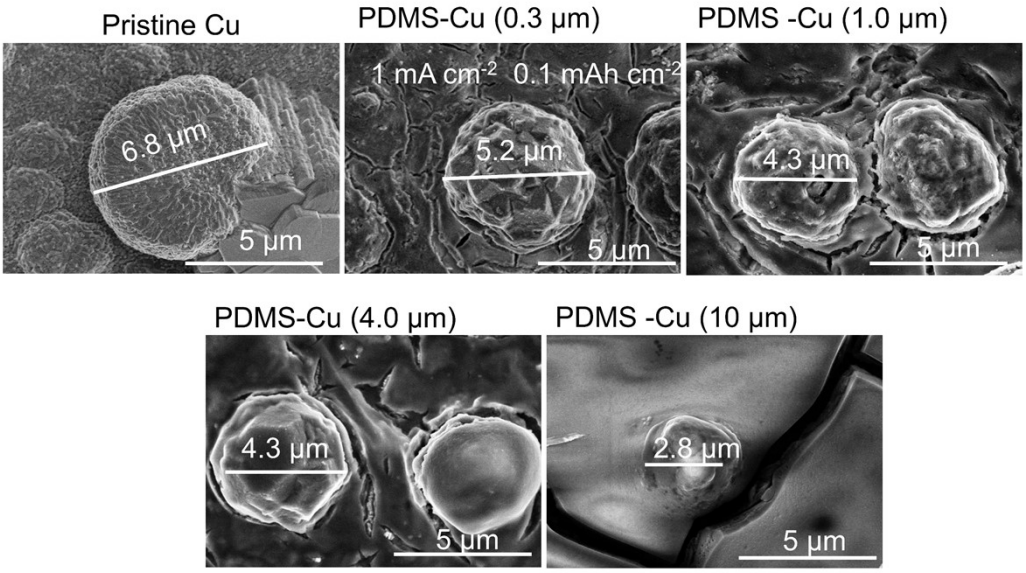

Fig. S7 The nuclei formed on the pristine Cu and PDMS-Cu (current density: 1 mA cm^{-2}, deposition capacity: 0.1 mAh cm^{-2})

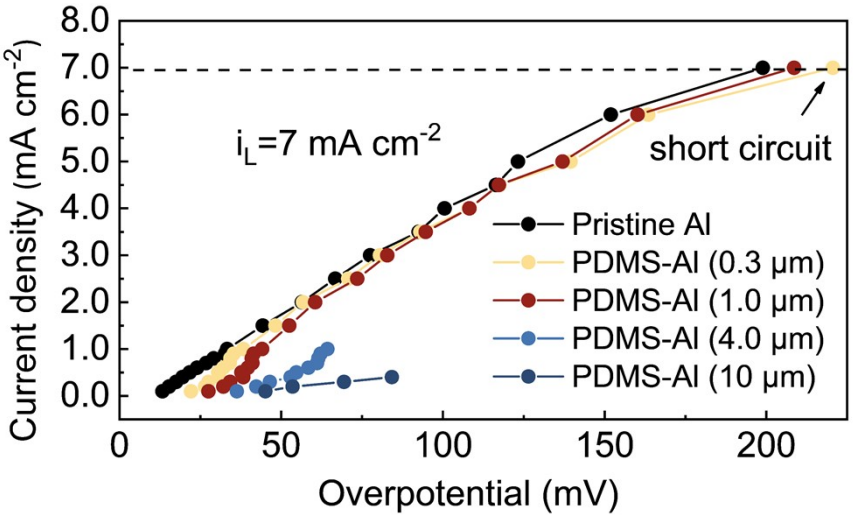

Fig. S8 Polarization curves of the symmetrical cells with pristine Al and PDMS-Al

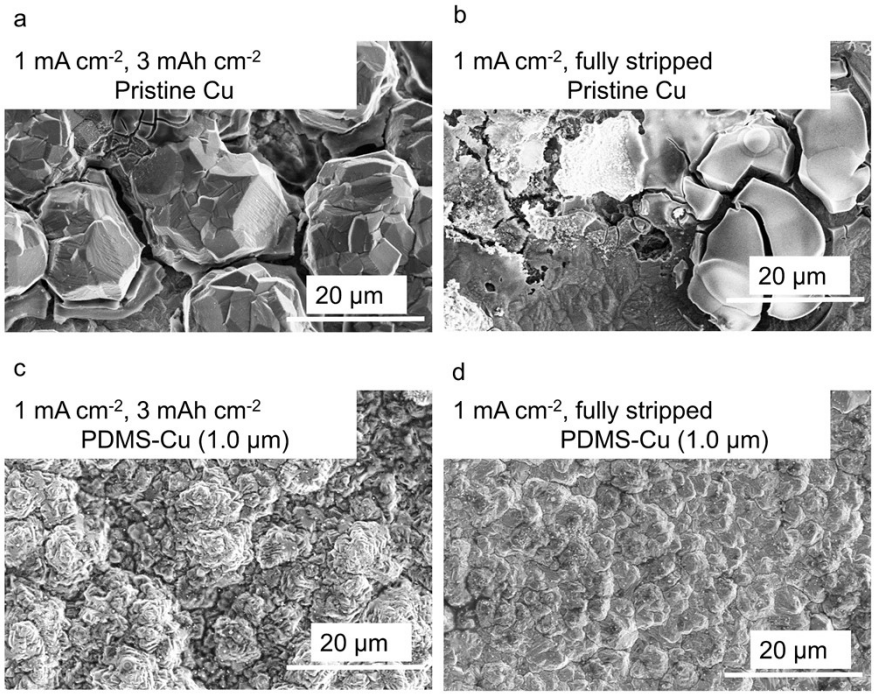

Fig. S9 The deposition and stripping morphology of Al on a,b) Cu, and c,d) PDMS-Cu (1.0 μm) (current density: 1 mA cm^{-2})

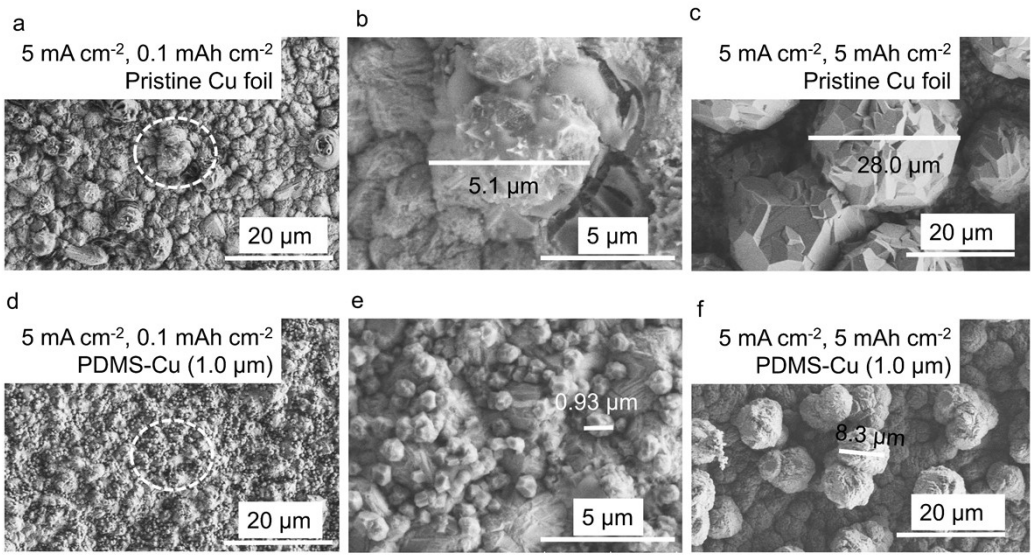

Fig. S10 The nucleation and deposition morphology of the Al under the current density of 5 mA cm^{-2} on the a-c) pristine Cu and d-f) PDMS-Cu (1.0 μm). b and e are the magnified areas in a and d.

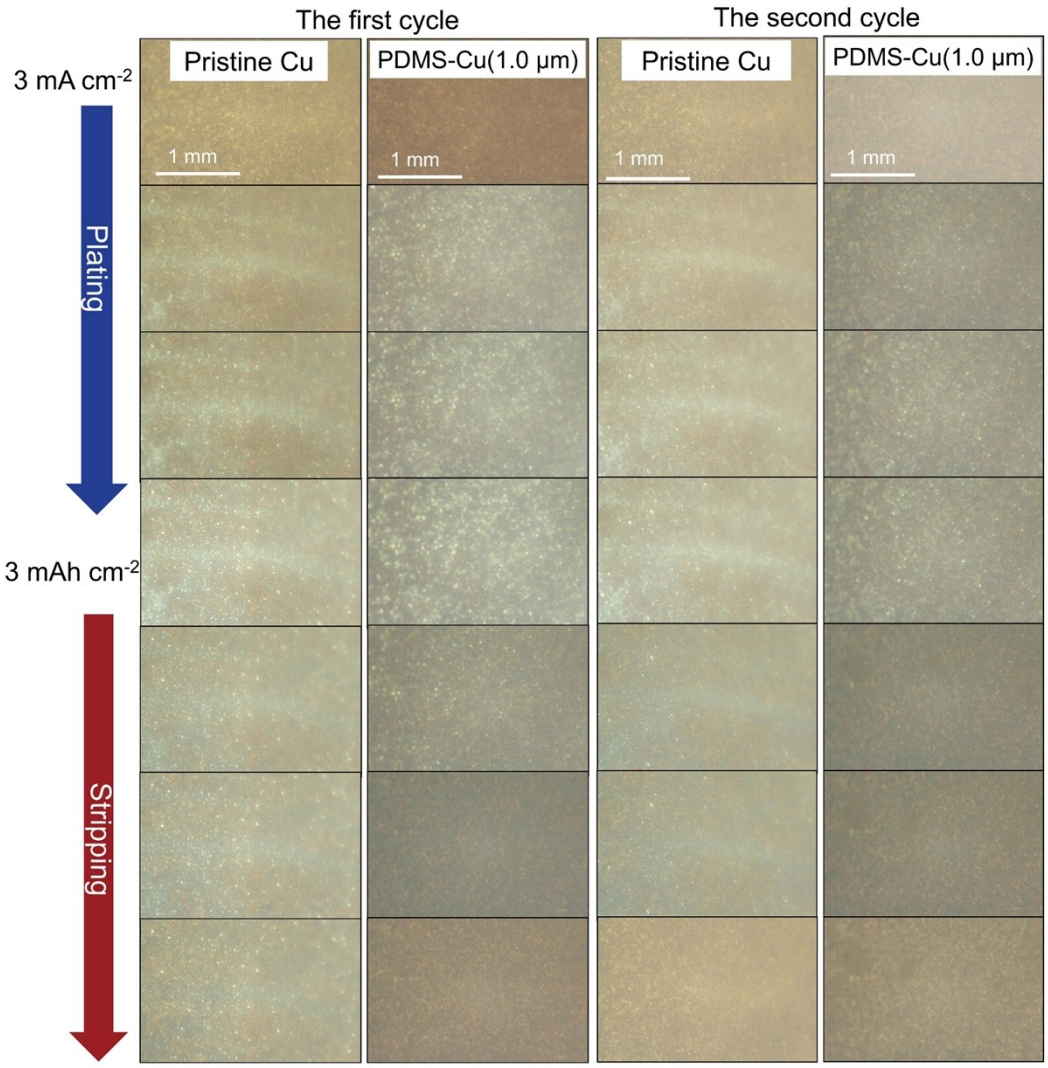

Fig. S11 *In-situ* optical microscopy images of the first and second plating and stripping cycle on the Cu or PDMS-Cu (1.0 μm) (current density: 3 mA cm^{-2}, plating capacity: 3 mAh cm^{-2}).

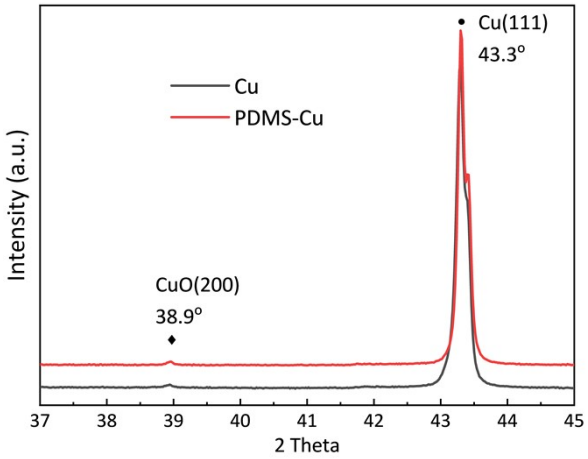

Fig. S12 The XRD patterns of the pristine Cu and PDMS-Cu (1.0 μm) before the *in-situ* XRD measurement.

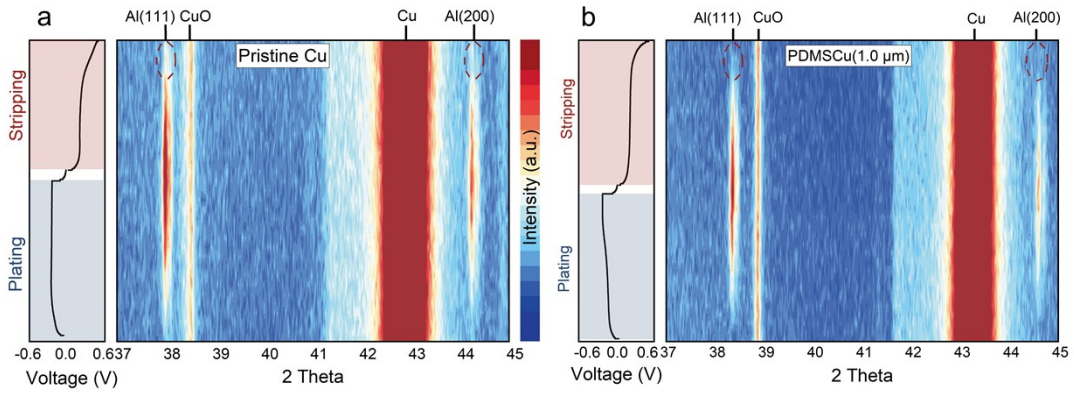

Fig. S13 *In-situ* XRD pattern and corresponding galvanostatic curves of the second plating and stripping cycle on the a) pristine Cu and b) PDMS-Cu (1.0 μm).

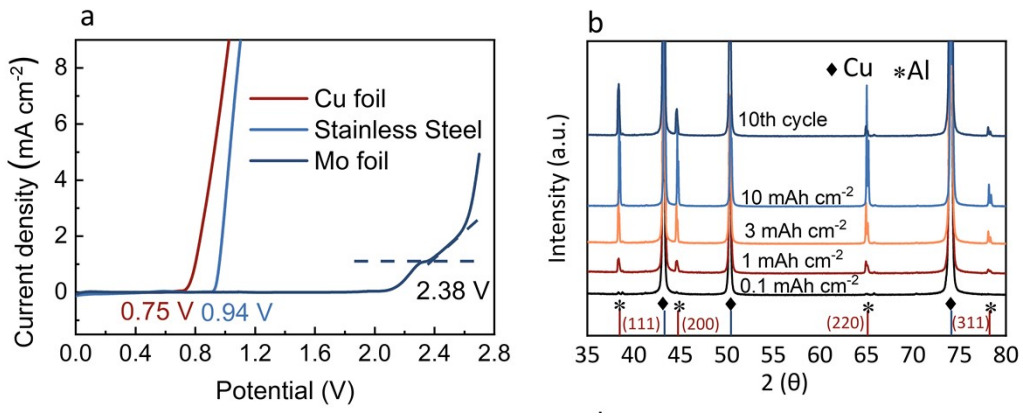

Fig. S14 a) Linear polarization curve of Cu foil, SS foil and Mo foil, b) XRD patterns of the electrodeposited Al on Cu foil with varied capacities and cycles.

Note: The Cu and SS electrodes do not show obvious corrosion current until the potential increases to 0.75 V and 0.94 V (*vs* Al^{3+}/Al). These potentials are higher than the upper limiting potential of the Al||Cu and Al||SS half cells (0.6 V), ensuring the stability of Cu and SS current collectors for Al deposition in the half cells. The Mo

foil shows a passivation plateau until 2.38 V, indicating stability under the potential of 2.38 V.

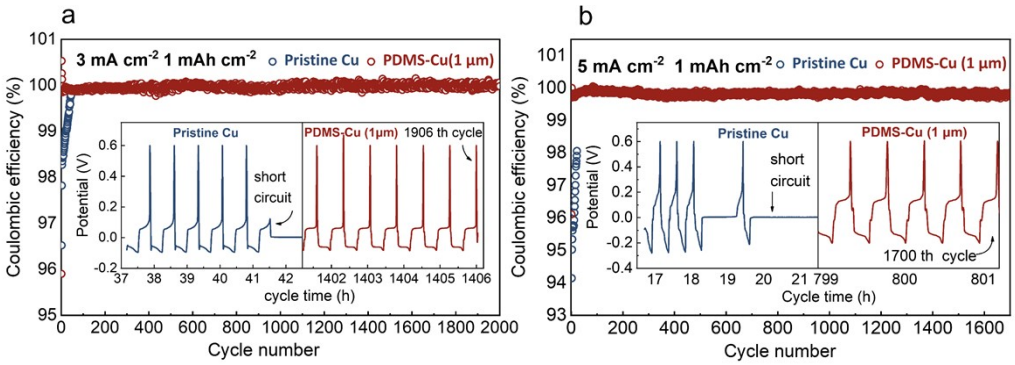

Fig. S15 The Coulombic efficiency of the Al||Cu half-cell with the pristine Cu or PDMS-Cu (1.0 μm) under a) 3 mA cm^{-2} and b) 5 mA cm^{-2} (deposition capacity: 1 mAh cm^{-2}).

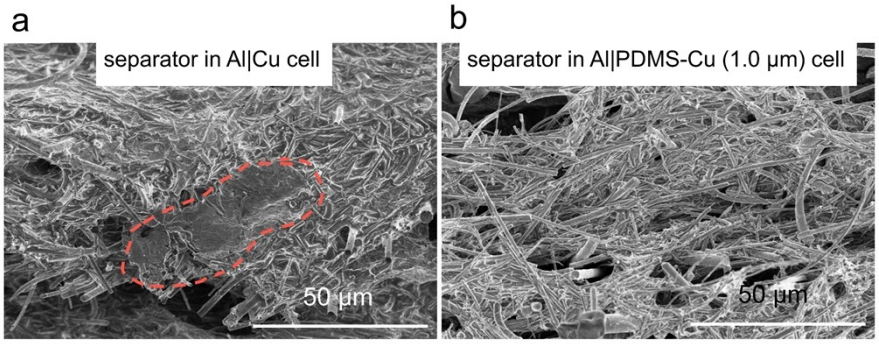

Fig. S16 The SEM images of the cross-section view of the glass fiber separator after 10 times of plate/stripe of the a) Al||Cu cell, and the b) Al||PDMS-Cu(1.0 μm).

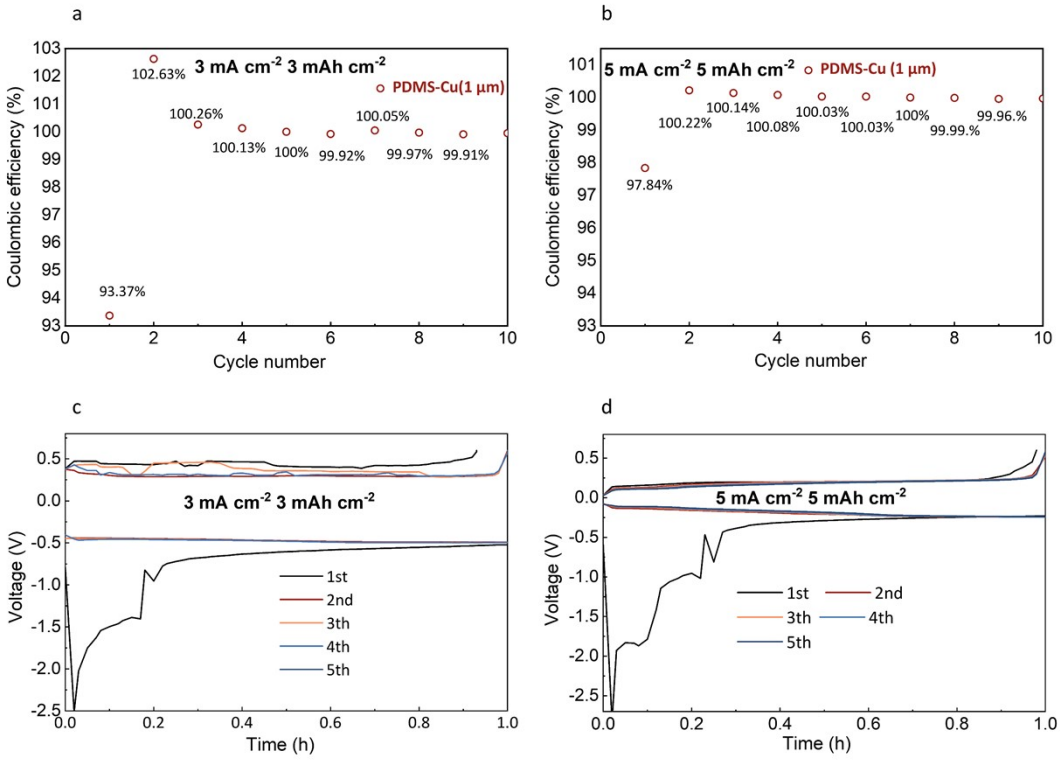

Fig. S17 a, b) The CEs of the first ten cycles for the Al||PDMS-Cu (1.0 μm) half cell under 3 mA cm^{-2}, 3 mAh cm^{-2} and 5 mA cm^{-2}, 5 mAh cm^{-2}. c, d) The first five plating and stripping curves of the Al||PDMS-Cu (1.0 μm) under the above conditions.

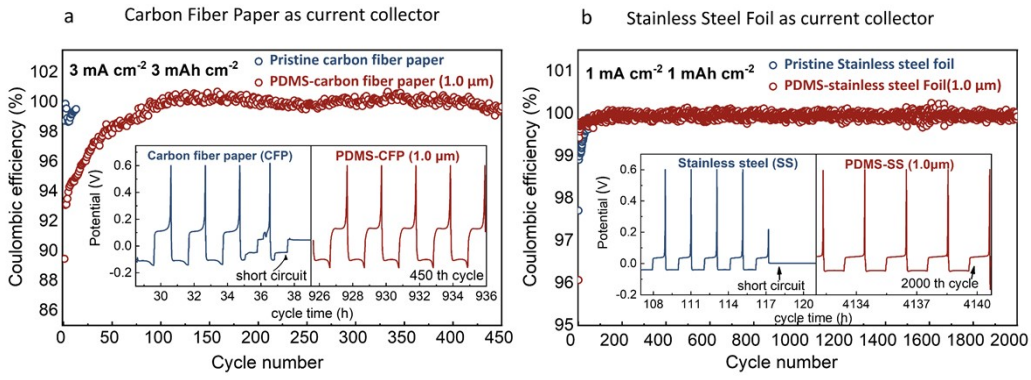

Fig. S18 The Coulombic efficiency of the a) Al||CFP and b) Al||SS cell with or without PDMS coating. The Al||CFP cells were cycled under the current density and capacity of 3 mA cm^{-2}, 3 mAh cm^{-2}, and the Al||SS cells were cycled under the current density and capacity of 1 mA cm^{-2}, 1 mAh cm^{-2}.

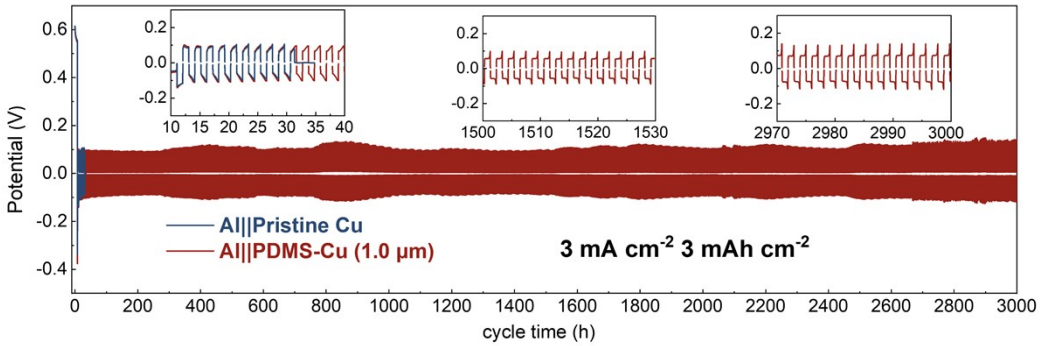

Fig. S19 Cycling performance of symmetrical cells with redeposited Cu or PDMS-Cu (current density: 3 mA cm^{-2}, capacity: 3 mAh cm^{-2}).

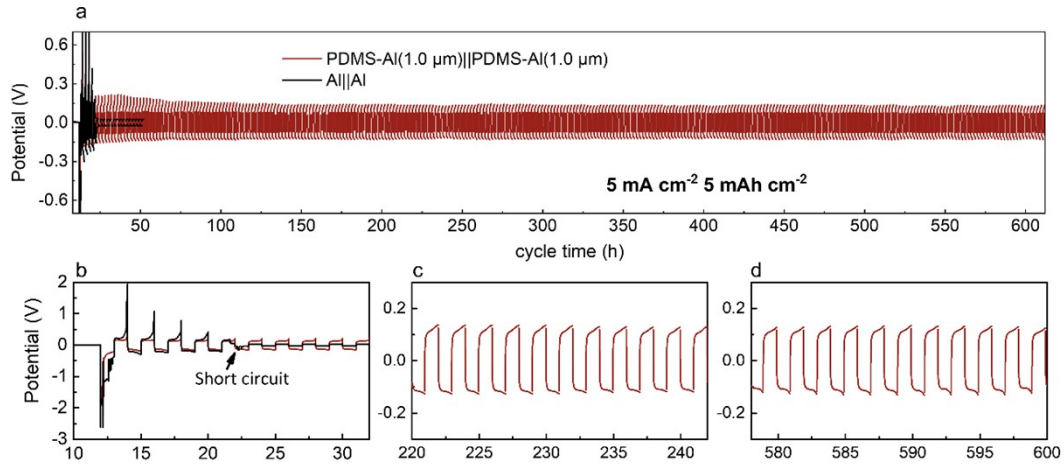

Figure S20 a) Cycling performance of symmetrical cells with pre-deposited Cu or PDMS-Cu (1.0 μm) under the current density of 5 mA cm^{-2} and capacity of 5 mAh cm^{-2}, b-d) The zoomed curves at different times.

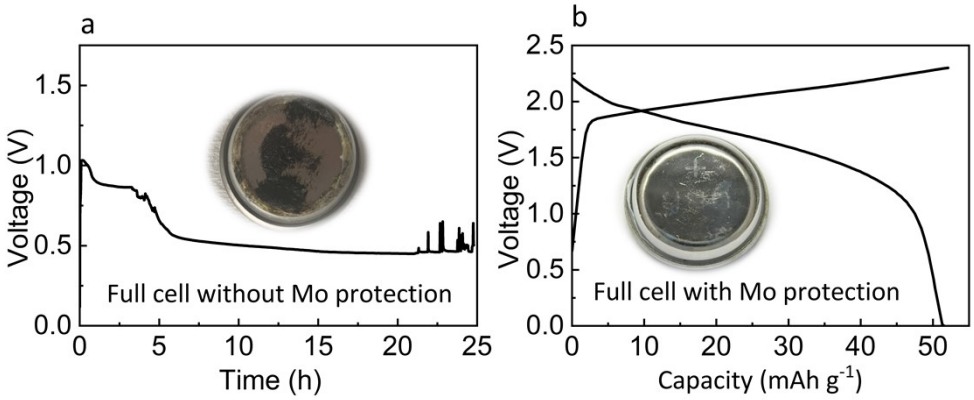

Fig. S21 a) Galvanostatic charging curve of the full cell without Mo protection (cathode material: artificial graphite), inset: SS cathode shell dissembled after the charging; b) Galvanostatic charging and discharging curve of the full cell with Mo foil protection, inset: SS cathode shell dissembled after 100 th cycling.

Note: The full cell using SS coin cell shells without protection displays long and fluctuated charging corrosion curves and cannot be cycled. The black corrosion patches are observed in the dissembled SS cathode shells. In contrast, using the Mo-protected SS coin cell case, the cell shows typical charging/discharging curves with the voltage plateau at 1.8-2.1 V and the cathode shell with Mo protection shows a clean and fresh surface after a long time cycling due to the high corrosion potential of Mo.

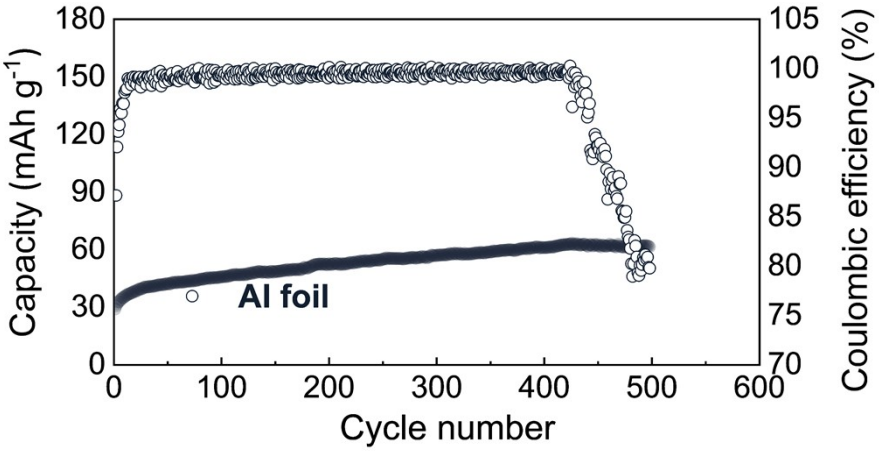

Fig. S22 The discharge capacity and the CE of the full cells with the artificial graphite cathode and Al foil anode.

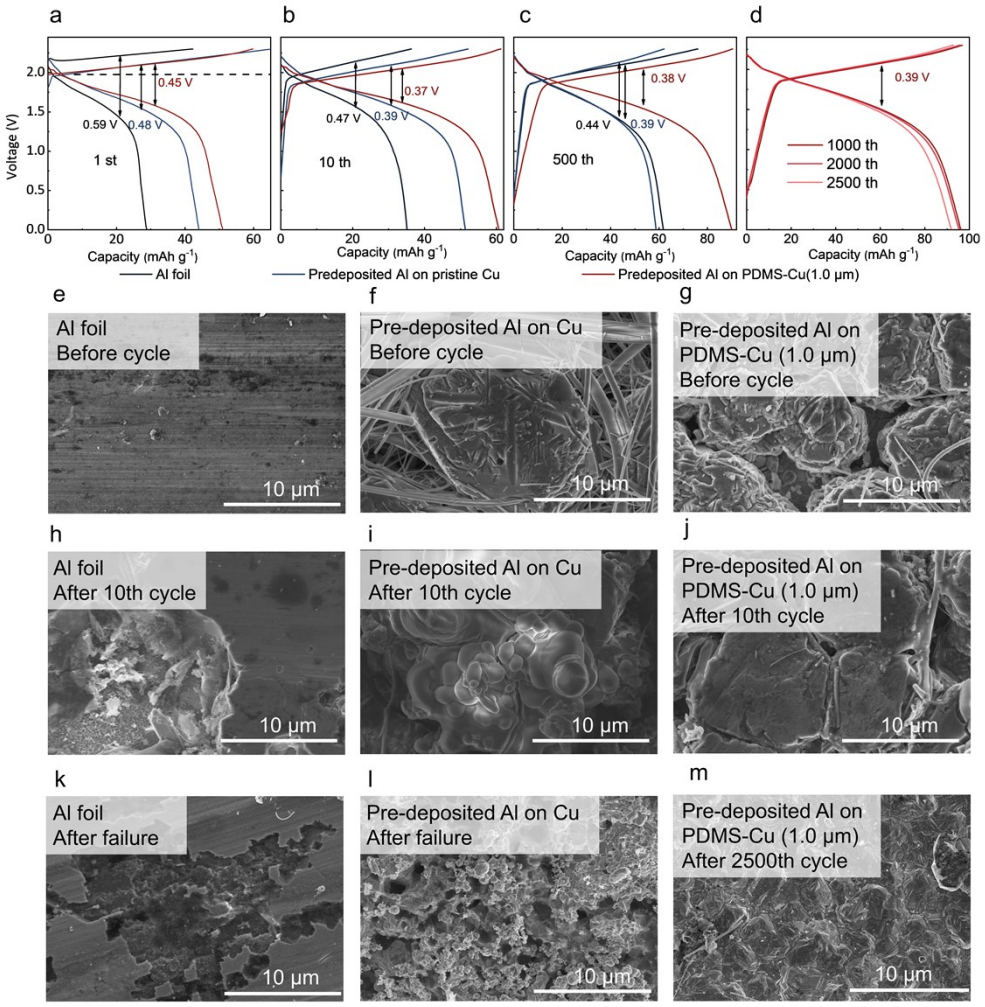

Fig. S23 a-c) The 1st, 10th and 500th galvanostatic charge and discharge curves of the full cells using the anodes of pure Al, pre-deposited Al on Cu, and pre-deposited Al on PDMS-Cu (1.0 μm); d) The 1000th, 2000th, and 2500th curves of the cell using the pre-deposited PDMS-Cu (1.0 μm); e-g) SEM image of the Al foil, the pre-deposited Al on Cu, and pre-deposited Al on PDMS-Cu (1.0 μm) before cycling; h-j) SEM image of the Al foil, pre-deposited Al on Cu and pre-deposited Al on PDMS-Cu (1.0 μm) after 10th cycles. k-m) SEM image of the Al foil after the battery failure

(660th cycle), the pre-deposited Al on Cu after the battery failure (1186 cycle), and pre-deposited Al on PDMS-Cu (1.0 μm) after 2500 cycles.

Table S1. The detailed CE, cycling number, and cycling time of the Al||Cu half cells

Deposition condition	Pristine Cu	PDMS-Cu (1.0 μm)
	Average CE, cycle number, cycling time	
3 mA cm^{-2}/1 mAh cm^{-2}	98.8%, 45 cycles, 34 h	99.9%, 2000 cycles, 1400 h
3 mA cm^{-2}/3 mAh cm^{-2}	97.8%, 8 cycles, 19 h	99.9%, 855 cycles, 1760 h
5 mA cm^{-2}/1 mAh cm^{-2}	96.1%, 22 cycles, 11 h	99.8%, 1700 cycles, 800 h
5 mA cm^{-2}/5 mAh cm^{-2}	96.6%, 5 cycles, 11 h	99.9%, 472 cycles, 930 h